RadioGraphics

Diffusely Enlarged Uterus: Evaluation with MR Imaging[1]

Aki Kido, MD • Kaori Togashi, MD • Takashi Koyama, MD • Toshihide Yamaoka, MD • Toshitaka Fujiwara, MD • Shingo Fujii, MD, PhD

CME FEATURE

See accompanying test at http://www.rsna.org/education/rg_cme.html

LEARNING OBJECTIVES FOR TEST 3

After reading this article and taking the test, the reader will be able to:

- List the various conditions that cause diffuse enlargement of the uterine corpus.
- Describe the MR imaging features of various conditions that manifest as diffuse uterine enlargement.
- Discuss the role of MR imaging in evaluation of various conditions that manifest as diffuse uterine enlargement.

Diffuse uterine enlargement is a common clinical finding. Because this abnormality can represent a physiologic manifestation, benign tumor, or malignancy, the diagnostic dilemma of a diffusely enlarged uterus can be challenging. Clinical findings can provide valuable information in regard to physiologic effects, pregnancy-related changes, and hormonal causes. Cytologic examination is essential for identification of cervical and endometrial malignancies. However, since preoperative histologic examination of myometrial lesions is not possible, preoperative distinction between benign and malignant conditions is frequently difficult. Imaging thus plays an important role in evaluation of myometrial lesions. In particular, magnetic resonance (MR) imaging allows specific diagnosis of several different lesions. Signal voids and prominent vessels at MR imaging are characteristic of vascular lesions. Adenomyosis and leiomyomas can be distinguished from other lesions with MR imaging, although a variety of unusual manifestations can be seen. MR imaging findings that allow distinction between leiomyoma and leiomyosarcoma have yet to be clearly established; however, invasion, hemorrhagic necrosis, or rapid growth is suggestive of malignancy. Endometrial stromal sarcoma tends to have distinct MR imaging features that allow differentiation from benign lesions.

Abbreviations: AVM = arteriovenous malformation, IUD = intrauterine device, RPOC = retained products of conception

Index terms: Arteriovenous malformations, uterine, 854.494 • Contraceptives and contraceptive devices, 854.463, 854.64 • Hormones, 854.64 • Placenta, abnormalities, 854.8249 • Pregnancy, 854.8269 • Tamoxifen, 854.64 • Uterine neoplasms, diagnosis, 854.30 • Uterus, anatomy, 854.92

RadioGraphics 2003; 23:1423–1439 • **Published online** 10.1148/rg.236035033

[1]From the Departments of Nuclear Medicine and Diagnostic Imaging (A.K., T.K., T.Y.), Diagnostic and Interventional Imageology (K.T., T.F.), and Obstetrics and Gynecology (S.F.), Graduate School of Medicine, Kyoto University, 54 Kawahara-cho, Shogoin, Sakyo-ku, Kyoto 606-8507, Japan. Presented as an education exhibit at the 2002 RSNA scientific assembly. Received February 19, 2003; revision requested March 20 and received May 5; accepted May 7. **Address correspondence to** A.K. (e-mail: *akikido@kuhp.kyoto-u.ac.jp*).

Introduction

Various conditions manifest as diffuse uterine enlargement, which represents one of the most common gynecologic findings. In adult women, the normal uterine corpus is approximately 5.0 cm in height (length), 5.0 cm in width, and 2.5 cm in anteroposterior thickness (1). This article discusses the uterus that is obviously larger than this size. Potential causes include physiologic changes, benign conditions, and malignant tumors. The myometrium is commonly involved, although the endometrium can also be involved. Imaging has an especially important role in evaluation of myometrial lesions, as histologic samples are not available for such lesions.

Uterine enlargement is typically first detected with physical examination or ultrasonography (US). US allows easy, noninvasive, cost-effective detection or confirmation of uterine enlargement. Nonetheless, US has limitations in displaying a global image of large tumors and in tissue characterization. Magnetic resonance (MR) imaging provides improved tissue contrast and better image quality, allowing determination of the precise location of a tumor and occasional specific diagnosis of lesions. MR imaging findings can allow noninvasive diagnosis of certain malignant tumors and benign conditions. However, the high cost and inconvenience associated with MR imaging can be prohibitive. US thus represents a primary diagnostic tool, whereas MR imaging assumes the role of a problem-solving tool. The use of computed tomography (CT) is mainly limited to evaluation of potential metastasis; this limitation is due to the risks associated with radiation exposure and the poor soft-tissue contrast, except for recognition of fat and calcification.

This article illustrates the MR imaging findings of various conditions that manifest as diffuse uterine enlargement and highlights important MR imaging and clinical findings that can help distinguish benign and malignant conditions. Specific topics discussed are physiologic findings, pregnancy-related changes, hormonal causes, vascular lesions, adenomyosis, neoplasms, and intrauterine devices.

Physiologic Findings

The average length and width of the uterus in women of reproductive age is 8 × 5 cm, whereas the average size in postmenopausal women is 5 × 2 cm (2). T2-weighted MR imaging clearly shows distinct zonal differentiation within the uterine corpus and cervix in women of reproductive age. The appearance and size of the uterus change in response to a variety of physiologic (ie, hormonal) effects, which include the menstrual cycle and aging (Fig 1).

Pregnancy-related Changes

With conception, the uterus gradually enlarges due to smooth muscle cell hypertrophy. The postpartum uterus temporarily exhibits a larger size than in the nonpregnant state. After dilation and curettage for termination of early-stage conceptions, the uterus maintains a normal size. Understanding the normal postpartum course and changes after dilation and curettage aids in identification of abnormal conditions related to pregnancy.

Postpartum Uterus

The mean uterine length in postpartum women within 24 hours after delivery is significantly longer than that in nonpregnant women (14 ± 1.4 cm vs 7 ± 1.4 cm, respectively) (3). The most significant decrease in the size of the uterine corpus occurs between 30 hours and 1 week after delivery (Table) (4).

The zonal appearance of the uterus shortly after vaginal delivery differs from that of the nonpregnant uterus (Fig 2). The endometrium displays a wide variety of signal intensities that represent fluid and blood products, which usually resolve after 1 week. The cervical stroma exhibits high signal intensity up to 30 hours after delivery and subsequently displays intermediate signal intensity (4). The myometrium is heterogeneous with engorged vessels of variable signal intensity for up to 30 hours after delivery. The junctional zone is usually not identifiable for approximately 6 weeks after delivery (4).

After cesarean section, the uterus can exhibit different postpartum findings than after vaginal delivery. It is common to observe a subacute

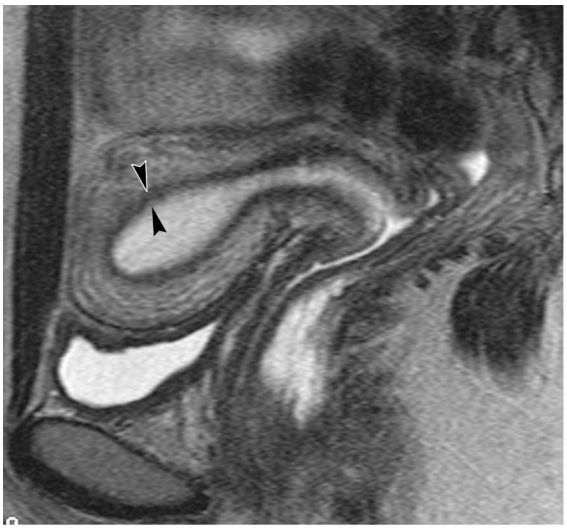

a.

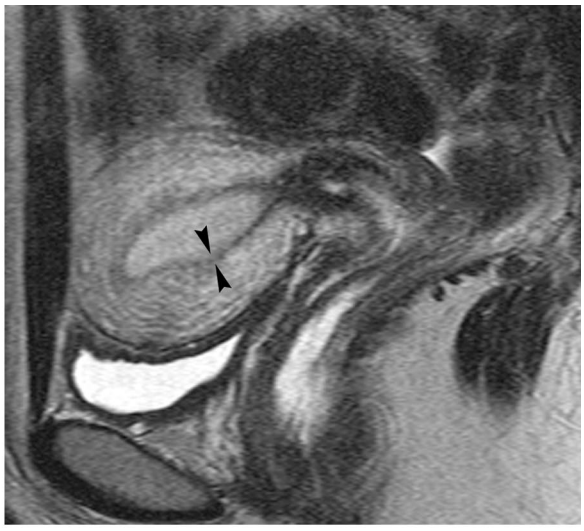

b.

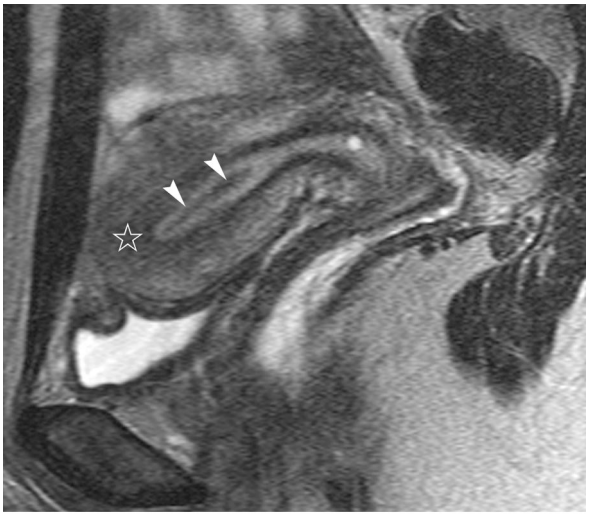

c.

Figure 1. Uterine changes during the menstrual cycle in a 31-year-old woman. **(a)** Sagittal T2-weighted image obtained during the periovulatory phase shows the anatomy of the three zones: endometrium, junctional zone (arrowheads), and outer myometrium. **(b)** Sagittal T2-weighted image obtained during the midsecretory phase shows increased thickness of the endometrium and myometrium. The signal intensity of the outer myometrium is increased. The thickness of the junctional zone (arrowheads) is significantly decreased. **(c)** Sagittal T2-weighted image obtained during the menstrual phase shows that the uterine corpus appears smaller than during the periovulatory and midsecretory phases. The zonal anatomy of the myometrium is ill defined and irregularly thick (☆). The low-signal-intensity band in the middle of the endometrium (arrowheads) represents menstrual blood.

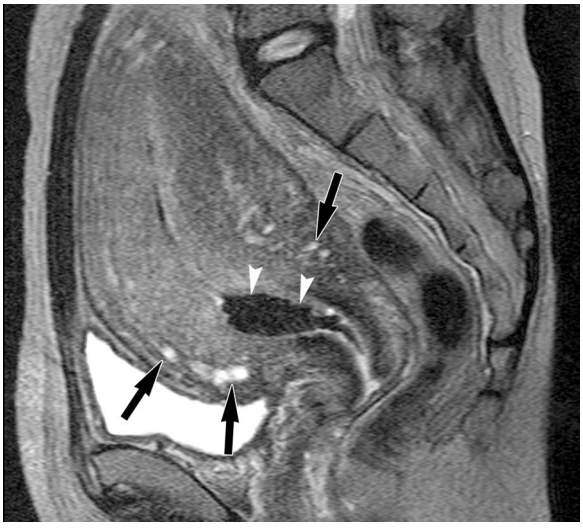

Figure 2. Appearance of the uterus in a 30-year-old woman 5 days after normal vaginal delivery. Sagittal T2-weighted image shows an enlarged uterus with dilated vessels (arrows) in the myometrium. The junctional zone is not identifiable. The regions of the endometrial cavity with marked low signal intensity (arrowheads) represent blood products.

Uterine Length after Childbirth

Time after Childbirth	Uterine Length (cm)	
	Mean	Range
30 h	13.8	11.8–15.9
1 wk	10.2	9.7–11.0
2 wk	8.6	7.9–8.8
6 wk	6.1	5.5–6.8
6 mo	5.0	3.9–6.0

Source.—Reference 4.

Figure 3. Appearance of the uterus in a 26-year-old woman after cesarean section at 31 weeks gestation. MR imaging was performed 8 days later for evaluation of cervical cancer. **(a)** Sagittal T1-weighted image shows a high-signal-intensity lesion (arrowheads) at the site of uterine incision, a finding consistent with a hematoma. **(b)** Sagittal T2-weighted image shows a bandlike appearance of the uterine incision (arrow) and the hematoma (black arrowheads). There are multiple dilated veins (white arrowheads) in the posterior wall.

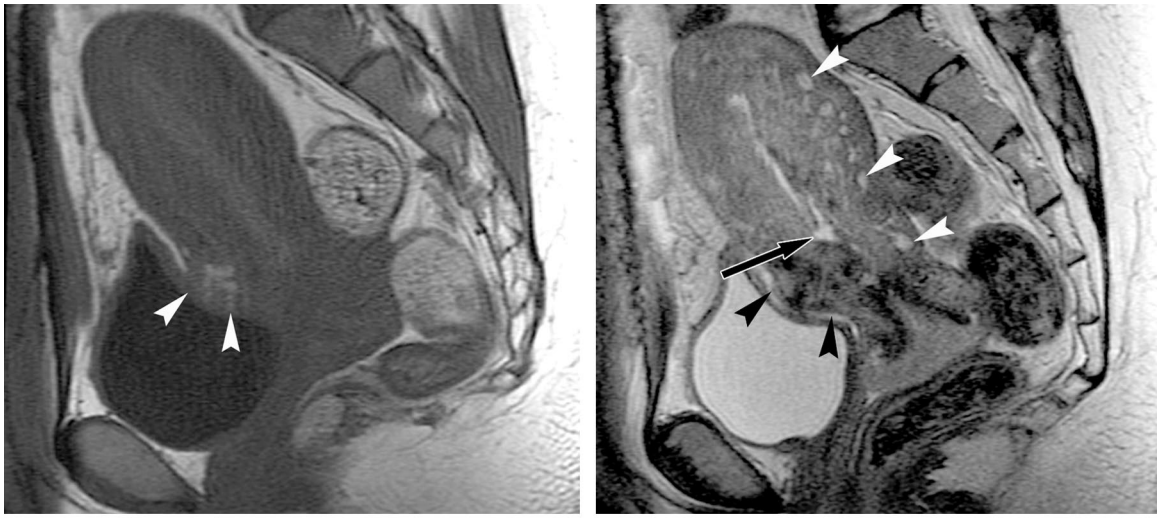

a. **b.**

hematoma at the uterine incision site, at the bladder flap, and within the endometrial cavity (Fig 3). Signal intensity varies according to the age of the hematoma. Uterine enlargement tends to persist longer after cesarean section than after vaginal delivery due to the delay in involution. Normal zonal anatomy is considered to reappear 6 months after cesarean section (5).

The lactation state can also influence uterine size after delivery. Uterine volume diminishes more rapidly in breast-feeding mothers (6). Three months after delivery, uterine size is much smaller in breast-feeding mothers than in bottle-feeding mothers (6).

Delay of Involution

Delay of involution is one of the most commonly encountered causes of a uterus larger than expected after delivery (Fig 4). The most common clinical presentation is abnormal postpartum bleeding. Many factors can result in subinvolution, such as fetal problems (excess amniotic fluid, multiple gestations), prolonged labor, intrauterine remnants (clots, placenta, debris), leiomyomas, uterine anomalies, and intrauterine infection. The clinical presentation and US are usually sufficient for differentiation between these entities. However, intrauterine hematoma, retained products of conception (RPOC), and endometritis are frequently indistinguishable at US, exhibiting thickened endometrium with heterogeneous signal intensity and intrauterine fluid (7,8).

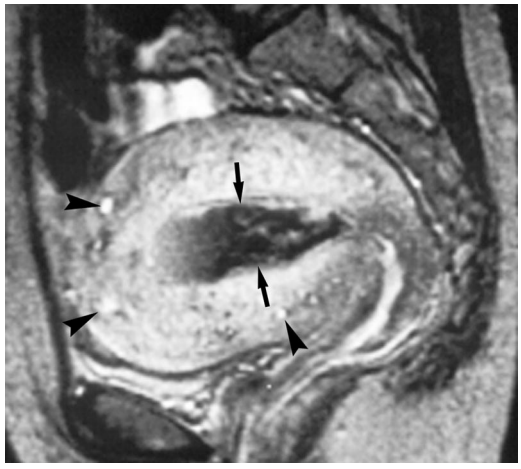

Figure 4. Delayed uterine involution 10 days after vaginal delivery in a 33-year-old woman. Sagittal T2-weighted image shows that the uterus is still enlarged. The myometrium has high signal intensity with prominent vessels (arrowheads). Low-signal-intensity fluid is seen in the endometrial cavity (arrows), a finding indicative of blood products.

Figure 5. Endometritis secondary to methicillin-resistant *Staphylococcus aureus* in a 31-year-old woman. Three weeks after cesarean section, the patient experienced septic shock. **(a)** Sagittal T2-weighted image shows the incision site for cesarean section in the anterior uterine wall (arrow). The uterus is enlarged with overall high signal intensity. The air (arrowhead) resulted from sanitization of the endometrial cavity. **(b)** Sagittal contrast material–enhanced T1-weighted image shows intense enhancement of the uterus with particularly prominent cervical enhancement (arrowheads). The cervix does not usually enhance so intensely unless it is significantly inflamed. The fluid seen in the endometrial cavity was found to be pus. **(c)** Sagittal T2-weighted image obtained 4 months after resolution of the endometritis shows decreased size of the uterus. The uterine position has changed from retroflexion to anteflexion. The zonal anatomy and the signal intensity of the myometrium have returned to normal. The diagnosis was confirmed with cultures of pus, which were positive for methicillin-resistant *S aureus*.

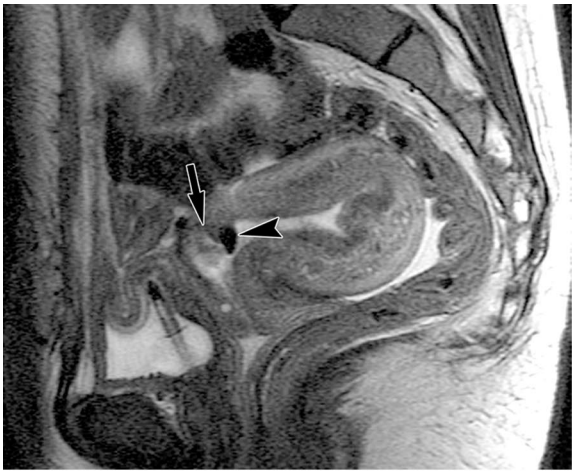

a.

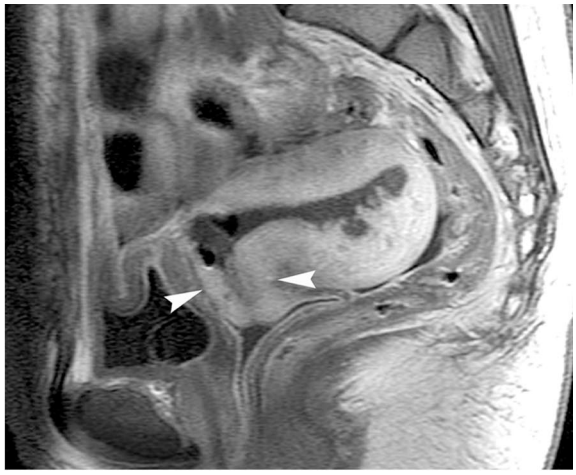

b.

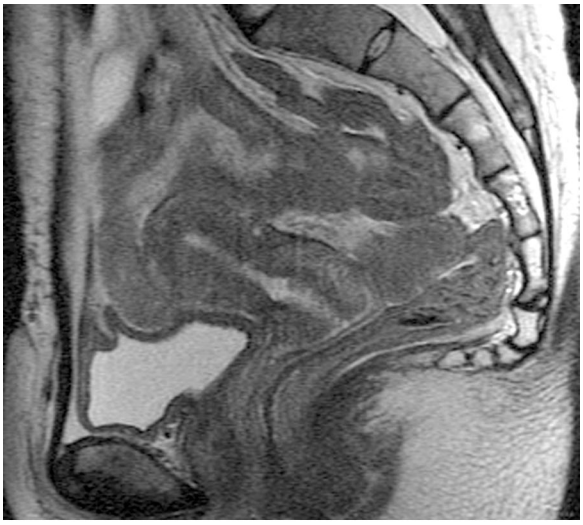

c.

MR imaging can allow distinction of such conditions in certain clinical settings. Hematomas demonstrate variable signal intensity, which reflects their maturity, and a lack of enhancement. In contrast, most cases of RPOC appear well enhanced (see next section). Intrauterine infection should be suspected when air bubbles are present in the uterine cavity (Fig 5). Homogeneous cervical enhancement can be another key point.

Retained Placenta and RPOC

Retained placental fragments (placenta accreta, placenta increta, placenta percreta) and RPOC involve retention of a portion of placental tissue in the uterine cavity after abortion or full-term delivery. Distinction of placenta increta or placenta percreta, which may require hysterectomy or embolization, from other types of retained placental tissue, which require only dilation and curettage, is clinically important. However, it is not always easy. In most cases, the typical presentation of retained placenta is a large and soft uterus, prolonged bleeding after delivery or dilation and curettage, and an elevated level of human chorionic gonadotropin.

Figure 6. Retained placenta in a 37-year-old woman. **(a)** Sagittal T2-weighted image shows an enlarged uterus with a high-signal-intensity subendometrial layer. A protruding lesion with high signal intensity (arrow) is seen in the uterine cavity, which is filled with low-signal-intensity blood (arrowheads). **(b)** Sagittal contrast-enhanced T1-weighted image shows marked enhancement of the protruding lesion (arrow), which indicates a retained placenta. The nonenhancing area in the lesion corresponds to a clot. Arrowheads = blood in the uterine cavity. Dilation and curettage performed after MR imaging demonstrated the presence of retained placenta.

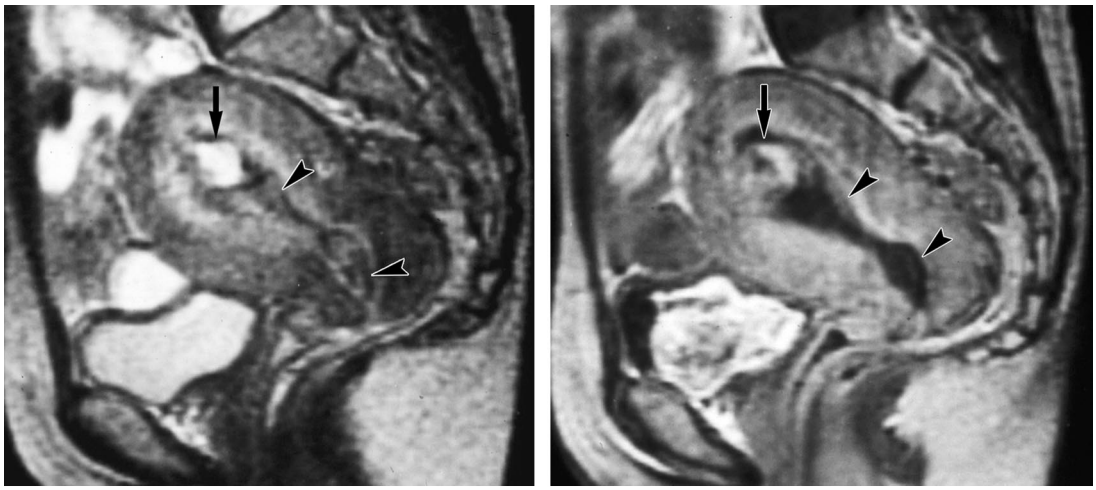

a. **b.**

The retained placental tissue exhibits high signal intensity on T2-weighted images and prominent enhancement on postcontrast images. Retained placental tissue can be associated with hematoma, which exhibits variable signal intensity on both T1- and T2-weighted images and is completely lacking in enhancement (Fig 6). However, occasionally the diagnosis presents a clinical challenge if the remaining placental tissue is too small to be clearly identified or necrotic without production of human chorionic gonadotropin. Reported imaging findings include either a polypoid mass protruding into the uterine cavity, which can be highly vascular or avascular according to the extent of degeneration, or numerous signal voids within the myometrium despite the absence of a cavitary lesion (9) (Fig 7).

Hormonal Causes

An enlarged uterus is frequently encountered in the presence of hormonal abnormalities. The most important hormonal factors resulting in uterine enlargement are increased serum levels of estrogen, progesterone, and gonadotropin. Uterine exposure to these hormones can be endogenous (eg, hormone-producing tumors) or exogenous.

The clinical presentation and history are important for identification of these conditions. Examples are a history of drug administration and abnormal or prolonged bleeding inconsistent with

Figure 7. RPOC in a 29-year-old woman who experienced acute massive vaginal bleeding 6 weeks after artificial abortion, which was performed due to a fatal anomaly of the fetus. **(a)** Sagittal T1-weighted image shows a slightly enlarged uterus with multiple serpentine signal voids (arrowheads) in the anterior wall and high-signal-intensity fluid (arrows) in the endometrial cavity. The latter finding is consistent with blood products. **(b)** Sagittal T2-weighted image shows numerous signal voids with ill-defined borders (arrowheads) in the anterior uterine wall. **(c)** Sagittal contrast-enhanced T1-weighted image shows ill-defined areas of enhancement (arrowheads) in the anterior uterine wall. However, no enhancing tissue protruding into the uterine cavity is seen. The preliminary diagnosis was arteriovenous malformation (AVM) or placenta increta. Hysterectomy was performed due to continued bleeding and the patient's refusal to undergo arterial embolization. Surgery revealed a mass in the anterior uterine wall, which was easily peeled away from the myometrium. Thus, the diagnosis of RPOC rather than placenta increta was established. This case illustrates the difficulty of differentiating RPOC from AVM or placenta increta with MR imaging.

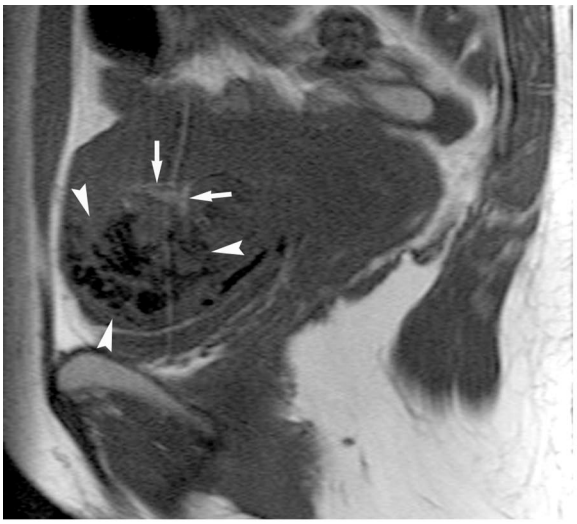

a.

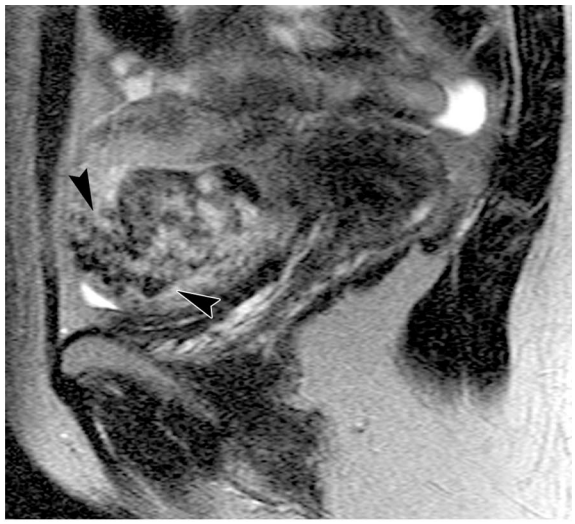

b.

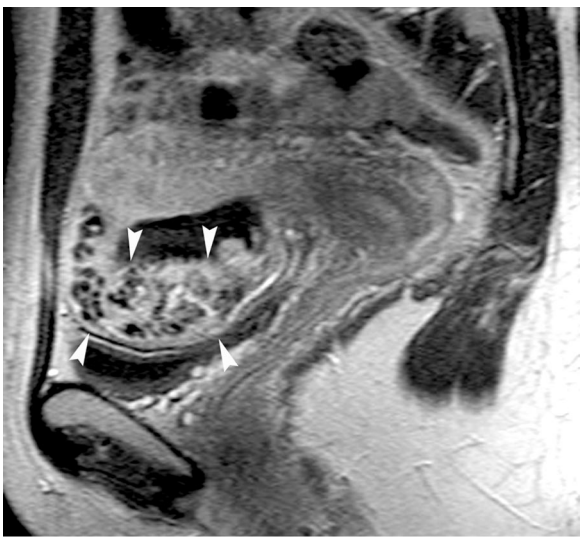

c.

patient age or menstrual cycle stage. Nonetheless, imaging findings can also be helpful. In conditions resulting from hormonal effects, an enlarged uterus has normal zonal anatomy, although the thickness or signal intensity of the endometrium and myometrium is abnormally increased.

Exogenous Hormones

Estroprogesterone.—Estroprogesterone (oral contraceptive pill) is used for both oral contraception and treatment of dysmenorrhea. Estroprogesterone administration can result in a myometrium that may appear swollen and globular with high signal intensity, whereas the endometrium can become atrophic due to smooth muscle hypertrophy, sinusoidal dilatation, and edema (10,11) (Fig 8). Myometrial swelling and endometrial atrophy are more pronounced in women taking higher concentrations of the hormone (10).

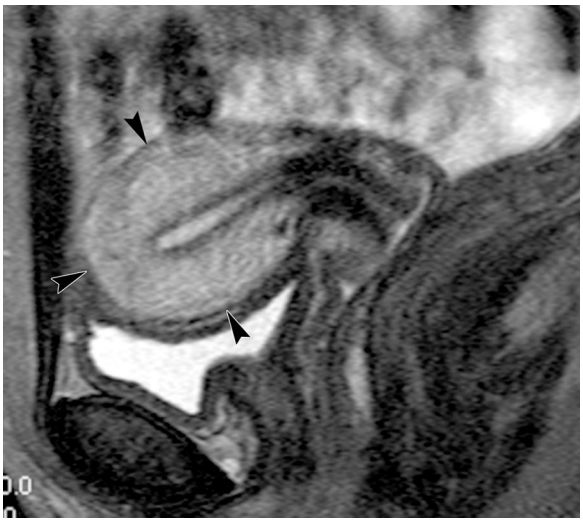

Figure 8. Uterine enlargement in a 22-year-old woman who had been taking estroprogesterone (oral contraceptive pills) for 3 months. Sagittal T2-weighted image shows a globular uterine corpus (arrowheads), a myometrium with increased signal intensity (higher than that of a normal uterus in a reproductive-age woman), and an atrophic endometrium.

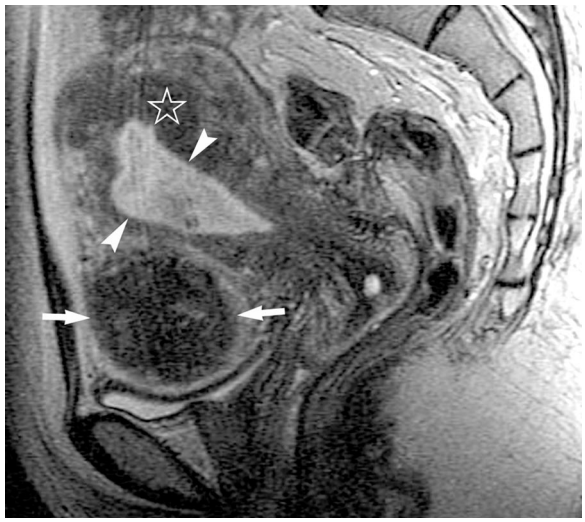

Figure 9. Endometrial hyperplasia in a 43-year-old woman who had been taking tamoxifen for 8 years for treatment of breast cancer with multiple bone metastases. Sagittal T2-weighted image shows thickened endometrium (arrowheads) and myometrium. The endometrium is thickened in a heterogeneous manner, a finding consistent with endometrial hyperplasia. The thickened junctional zone in the posterior uterine wall (☆) is indicative of adenomyosis. A leiomyoma (arrows) is present in the anterior uterine wall. Endometrial hyperplasia was demonstrated at histologic examination.

Tamoxifen.—The uterus can exhibit prominent enlargement and severe zonal anatomy distortion with use of tamoxifen, which is widely used for breast cancer treatment (12). Tamoxifen also acts as a weak estrogen agonist for postmenopausal endometrial tissue; women taking tamoxifen have a significantly larger uterus and can exhibit endometrial abnormalities, such as hyperplasia, polyps, and carcinoma (12). At US, endometrial hyperplasia should be suspected whenever the endometrium is more than 10 mm thick, especially in postmenopausal patients (13). However, the US appearances of endometrial hyperplasia, polyps, and cancer are all the same and thus are not diagnostic (14). MR imaging findings of multiple cysts or latticelike enhancement of the endometrium on postcontrast images are encountered frequently in tamoxifen-ingesting patients and favor a benign diagnosis (12) (Fig 9). However, even MR imaging findings are not sufficiently specific to obviate histologic study of thick endometrium.

Endogenous Hormones

Hormone-producing tumors should be considered when both an enlarged uterus and an adnexal mass are present. Uterine imaging findings are nearly identical to those observed with tamoxifen use. Granulosa cell tumors are the most commonly encountered tumor, but other gonadal stromal tumors and a variety of other ovarian neoplasms have also been associated with functioning stromal tissue (15) (Fig 10). Malignant tumors are more common than benign tumors. The most common tumors are surface epithelial–stromal carcinomas, particularly those with mucinous and endometrioid differentiation, and metastatic carcinomas, especially from the large intestine.

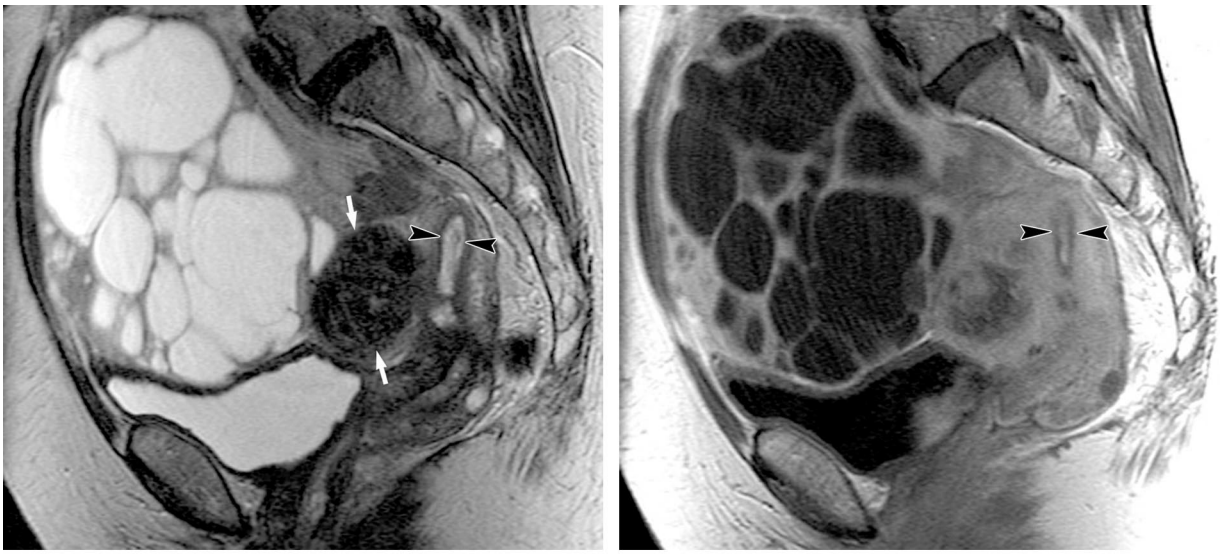

a. b.

Figure 10. Granulosa cell tumor in a 65-year-old woman with abnormal genital bleeding and an estradiol level of 36 pg/mL (normal level, <16 pg/mL). **(a)** Sagittal T2-weighted image shows that the uterus is slightly enlarged for the patient's age with thickened endometrium (arrowheads). A subserosal leiomyoma (arrows) is present in the anterior wall. A large ovarian tumor with multiple cystic components is present anterior to the uterus. **(b)** Sagittal contrast-enhanced T1-weighted image shows marked enhancement of the endometrium (arrowheads), which is indicative of cystic hyperplasia. The ovarian wall and septa also demonstrate marked enhancement. The estradiol level returned to normal after surgery. Histologic examination demonstrated a granulosa cell tumor.

Vascular Lesions

A bulky uterus may be encountered secondary to abnormal vascular lesions. Prominent gonadal, parametrial, and myometrial vasculature, with or without arteriovenous shunting, characterizes such lesions. Uterine enlargement can result from prominently engorged vessels or myometrial edema (16). Although angiography is the standard of reference for diagnosing AVMs and other vascular abnormalities, MR imaging and MR angiography are emerging as effective modalities for noninvasive evaluation of such conditions.

Arteriovenous Malformation

An AVM is a distinct disease entity composed of a tangle of vessels that possess the histologic characteristics of both arteries and veins with lack of an intervening capillary network. Usually, an AVM is first suspected at examination with gray-scale US, which demonstrates multiple anechoic structures with a serpentine contour within the myometrium. Color Doppler images exhibit intense juxtaposed signals with low-resistance flow (16). MR imaging allows noninvasive diagnosis of AVMs on identification of a cluster of serpentine flow-related signal voids within a thick myometrium (16).

As AVMs are probably acquired following trauma, they can be associated with a variety of conditions, such as normal uterine pregnancy, miscarriage, abortion, ectopic pregnancy, placental polyps, endometrial cancer, and choriocarcinoma (16). Images suggesting the diagnosis of AVM should be evaluated carefully in association with cytologic and clinical information, such as the serum level of β–human chorionic gonadotropin, which is helpful in diagnosis of pregnancy-related conditions and gestational trophoblastic disease (16,17). If a pregnancy-related or tumor-associated AVM is definitively excluded, uterine AVMs can be treated with transcatheter embolization. Contrast-enhanced dynamic MR angiography can be useful for both planning therapeutic embolization and monitoring the effects of treatment (18).

Pelvic Congestion Syndrome

Pelvic congestion syndrome involves vague symptoms, including chronic pelvic pain, that are associated with dilated ovarian veins and pelvic varices resulting from left renal vein reflux (19,20)

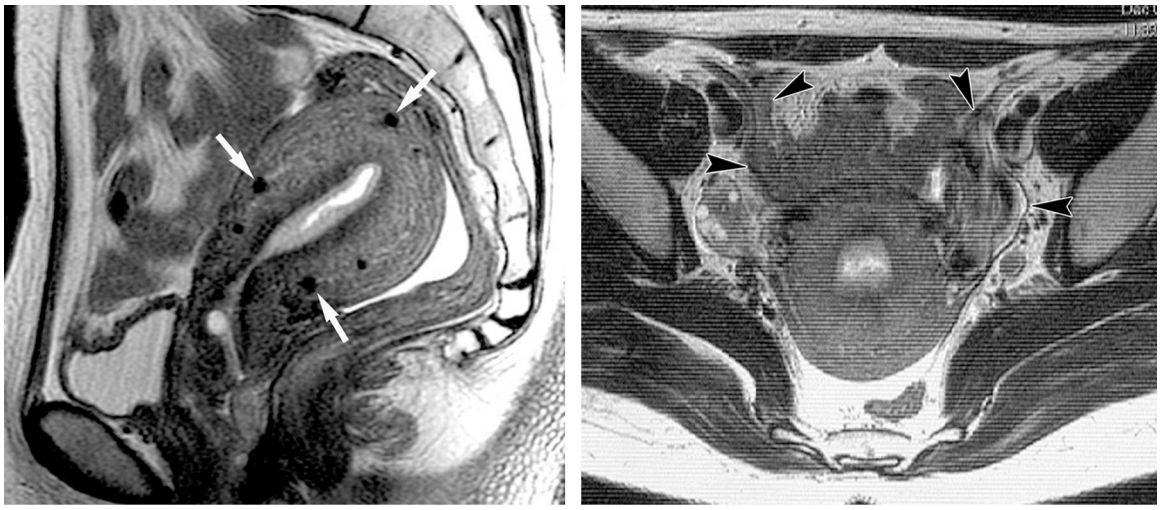

a. **b.**

Figure 11. Pelvic congestion syndrome in a 35-year-old woman (gravida 2, para 2) with chronic lower abdominal pain, hypermenorrhea, and abnormal genital bleeding. **(a)** Sagittal T2-weighted image shows thickened myometrium with numerous dilated signal voids (arrows). **(b)** Axial T2-weighted image shows multiple dilated veins (arrowheads) around the uterus. Abdominal CT demonstrated retrograde filling of the ovarian veins. Pelvic congestion syndrome was suspected on the basis of both the clinical presentation and the imaging findings. The symptoms and uterine size decreased after embolization of the ovarian veins.

(Fig 11). The uterus is enlarged, usually with engorged arcuate vessels in the myometrium. CT and MR imaging findings of this condition include varicose veins around the uterus and ovaries with retrograde filling of ovarian veins. Some researchers consider ovarian veins with diameters greater than 5 mm pathognomonic for pelvic congestion syndrome (19), but this diagnostic criterion is not universally accepted. At present, invasive angiography is considered the primary diagnostic tool in patients with clinical symptoms. Given the benign nature of this condition, noninvasive MR angiography appears to be a promising diagnostic alternative. MR angiography can clearly demonstrate abnormal venous flow, which can guide subsequent invasive angiography and venous embolization.

Adenomyosis

The term *adenomyosis* refers to benign invasion of the endometrium into the myometrium with reactive overgrowth of the musculature. US illustrates the lesion as decreased echogenicity or heterogeneity of the myometrial region with small embedded cysts (21). MR imaging demonstrates diffuse or focal widening of the junctional zone, with a width of greater than 12 mm considered to be highly associated with adenomyosis (21). The uterus is enlarged with diffuse or focal low signal intensity on T2-weighted images.

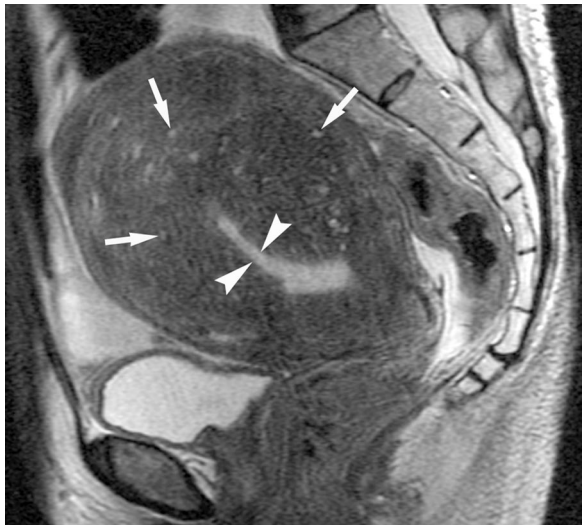

Figure 12. Adenomyosis. Sagittal T2-weighted image shows indistinct zonal anatomy. Widening of the junctional zone is clearly seen in the region around the distorted endometrium (arrowheads). The myometrium has decreased signal intensity with tiny spots of high signal intensity (arrows).

Bright spots are observed on T1- or T2-weighted images in lesions of adenomyosis (22) (Fig 12). The bright foci correspond to heterotopic endometrial tissue, cystic dilatation of endometrial glands, or hemorrhagic foci. At US, such areas appear as small myometrial cysts within myometrial regions of decreased echogenicity or heterogeneity (21).

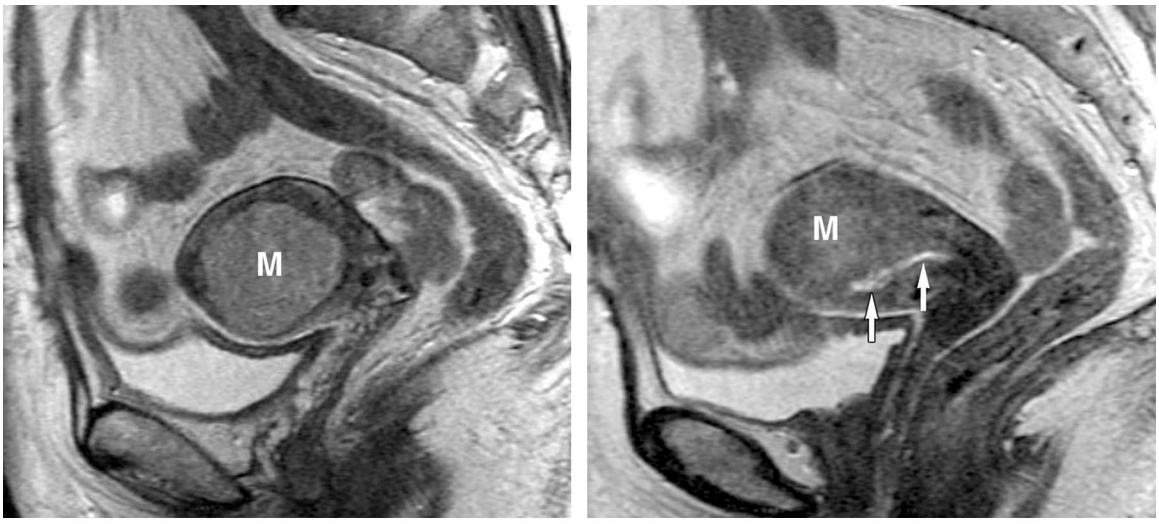

a. **b.**

Figure 14. Adenocarcinoma arising from adenomyosis in a 71-year-old woman. **(a)** Sagittal T2-weighted image shows a mass *(M)* in the submucosal area of the posterior region. The mass is hyperintense relative to the myometrium. **(b)** Sagittal T2-weighted image obtained 1 cm lateral to **a** shows that the margins of the mass *(M)* are indistinct at its periphery. Arrows = endometrium. Histologic examination of the surgical specimen revealed endometrioid adenocarcinoma arising from adenomyosis.

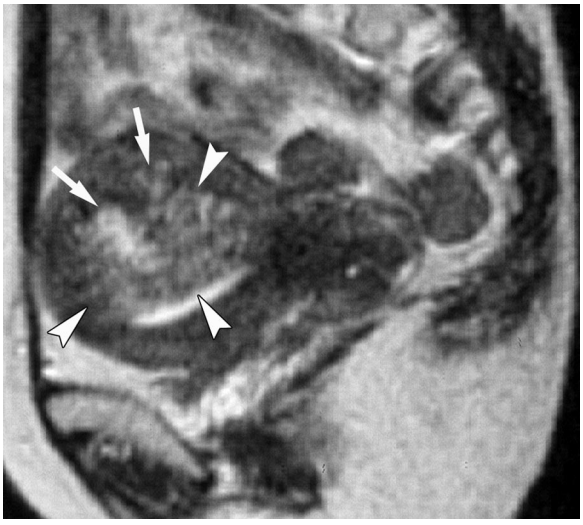

Figure 13. Focal adenomyosis in a 49-year-old woman. Sagittal T2-weighted image shows a heterogeneous area of high signal intensity (arrowheads) within the myometrium that protrudes into the uterine cavity. The interface between the lesion and the myometrium is indistinct. Fine hyperintense striations (arrows) extend into the myometrium; this appearance is an extreme example of pseudowidening of the endometrium.

Striations of high signal intensity radiating from the endometrium directly correspond to benign endometrial invasion. The term *pseudowidening of the endometrium* refers to the blending of such fine striations with the myometrium, resulting in an appearance that can resemble invasion by uterine malignancy (Fig 13). Another point of caution is that endometrial adenocarcinoma can arise from ectopic endometrium in adenomyosis and manifest as a bright spot larger than other surrounding lesions (23) (Fig 14).

Neoplasms

Neoplasms are probably the most common and, at the same time, the most important category of lesions in evaluation of an enlarged uterus. Diffuse neoplastic uterine enlargement typically exhibits two patterns: multiple nodules and extensive replacement of the myometrium by tumor. Mesenchymal or myometrial masses are difficult to evaluate with histologic examination, whereas epithelial tumors are easily evaluated with such studies.

Multiple Nodules

Neoplasms that typically manifest as multiple nodules include leiomyoma, leiomyosarcoma, and endometrial stromal sarcoma. MR imaging findings of uterine leiomyomas are well established (24). In contrast, reports concerning other mesenchymal tumors are very limited, which thus hinders effective evaluation of an enlarged uterus.

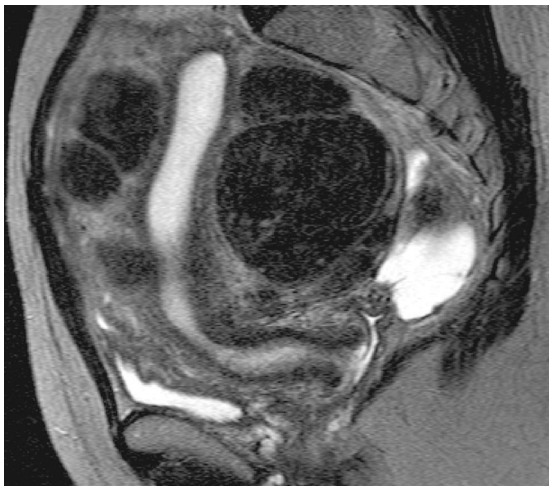

Figure 15. Multiple leiomyomas in a 44-year-old woman. Sagittal T2-weighted image shows a diffusely enlarged uterus with multiple leiomyomas. Each leiomyoma has clear margins and distinct low signal intensity.

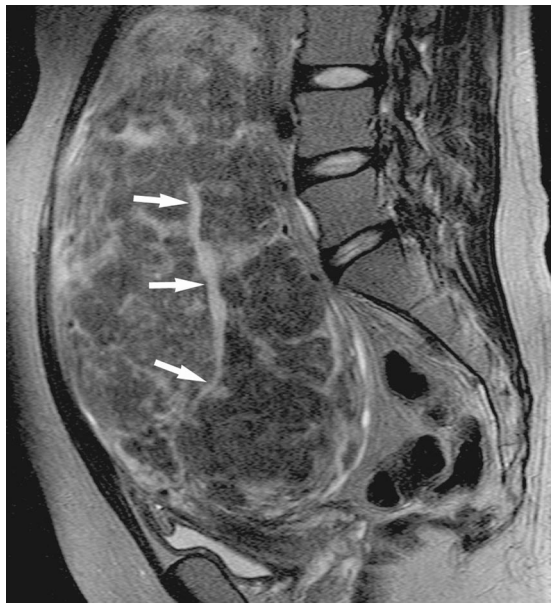

Figure 16. Diffuse leiomyomatosis in a 31-year-old woman. Sagittal T2-weighted image shows a prominently enlarged uterus with innumerable leiomyomas that appear to blend with one another. The endometrium (arrows) is markedly elongated and distorted by multiple submucosal nodules.

Leiomyoma.—Leiomyomas are by far the most common uterine tumor, frequently manifesting as diffuse uterine enlargement with multiple nodules. Consistent with their benign nature, leiomyomas exhibit a "pushing" border and a rounded appearance. Leiomyomas typically display distinct low signal intensity with a speckled appearance on T2-weighted images (24) (Fig 15). Although leiomyomas can demonstrate variable appearances due to the presence of edema and hyaline, cystic, and red degeneration, knowledge of the MR imaging characteristics of such variations can aid in differentiating leiomyomas from other mesenchymal tumors.

Intravenous Leiomyomatosis.—Intravenous leiomyomatosis is a rare condition characterized by leiomyomas remarkable for growth of smooth muscle cells into venous vasculature, although they are otherwise unremarkable. Convoluted, wormlike masses growing within veins, often extending into the broad ligament, other pelvic veins, the inferior vena cava, or even the heart (25), are the hallmark features of intravenous leiomyomatosis.

Diffuse Leiomyomatosis.—Diffuse leiomyomatosis is defined as the presence of innumerable small leiomyomas that produce symmetrical enlargement of the uterus, replacing most of the uterine parenchyma (Fig 16). MR imaging demonstrates innumerable nodules that blend with one another and replace the uterine parenchyma to near completion (25). Such nodules display low to intermediate signal intensity on T2-weighted images. All reported cases necessitate hysterectomy regardless of the patient's reproductive age, as hormonal treatments have not proved helpful. Nonetheless, uterine artery embolization might be an effective alternative treatment for this benign condition. Definitive diagnosis of this condition with MR imaging might allow consideration of uterine artery embolization as a treatment option for women of reproductive age.

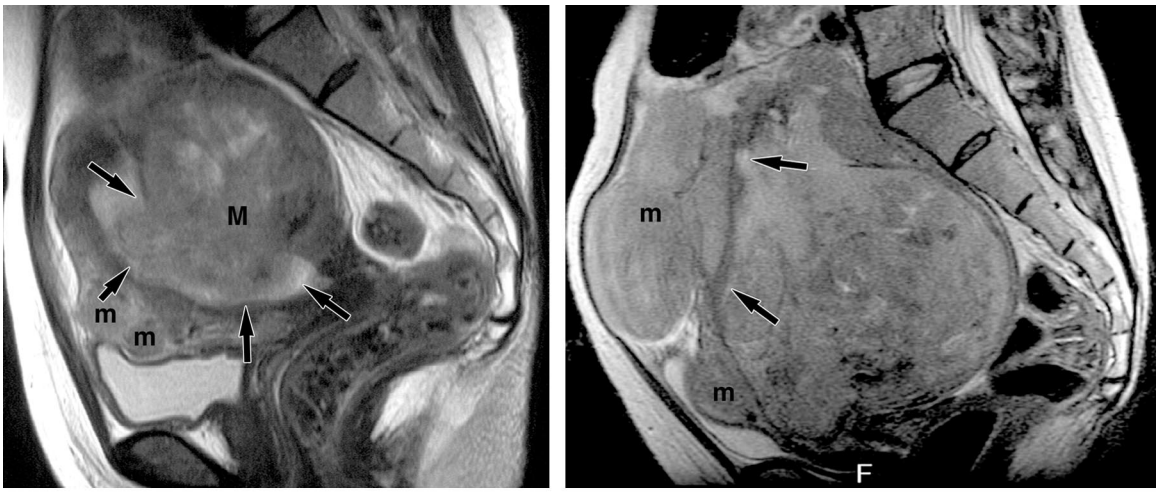

a. **b.**

Figure 17. Leiomyosarcoma in a 44-year-old woman. **(a)** Sagittal T2-weighted image shows a tumor *(M)* with slightly high signal intensity and irregular margins. The tumor protrudes from the posterior myometrium into the endometrial cavity (arrows). Small leiomyomas *(m)* with clear margins are present in the anterior wall. **(b)** Sagittal T2-weighted image, obtained 3 months later after the patient experienced rapidly progressing abdominal fullness, shows an irregularly shaped uterus that has clearly increased in size. The tumor occupies the endometrial cavity (arrows). The nodules *(m)* in the anterior wall also demonstrate remarkable increase in size.

Leiomyosarcoma.—Leiomyosarcomas are very rare tumors that are often initially misdiagnosed as leiomyomas. Rapid growth and extensive metastasis are frequently encountered with leiomyosarcomas. As the disease progresses, which can occur with extreme rapidity after an initial manifestation, leiomyosarcomas appear as either a prominently enlarged uterus with multiple sarcomatous nodules or extensive invasion (Fig 17). Reported MR imaging findings are variable and include a lobulated mass of high signal intensity on T2-weighted images, a sharply marginated mass of low signal intensity that closely resembles a leiomyoma, or a mass with focally infiltrative margins (26). Signal intensity is not a reliable indicator of malignancy. Detection of scattered foci of hemorrhage or necrosis can serve as a clue for diagnosis of leiomyosarcoma, as such findings can reflect coagulative necrosis, which should raise suspicion for leiomyosarcoma. At MR imaging, such necrotic areas are seen as areas of slightly high signal intensity on T1-weighted images and heterogeneous areas on T2-weighted images.

Diffuse Myometrial Involvement

Diffuse myometrial involvement is usually observed with malignant tumors. Although most lesions in this category diffusely involve the uterus, occasionally nodular involvement can be observed with these lesions.

Hematologic Malignancies.—The uterine cervix and corpus are rarely the primary site for leukemia or lymphoma. When uterine lymphoma does occur, the most common manifestation is diffuse symmetrical uterine enlargement with relatively high signal intensity on T2-weighted

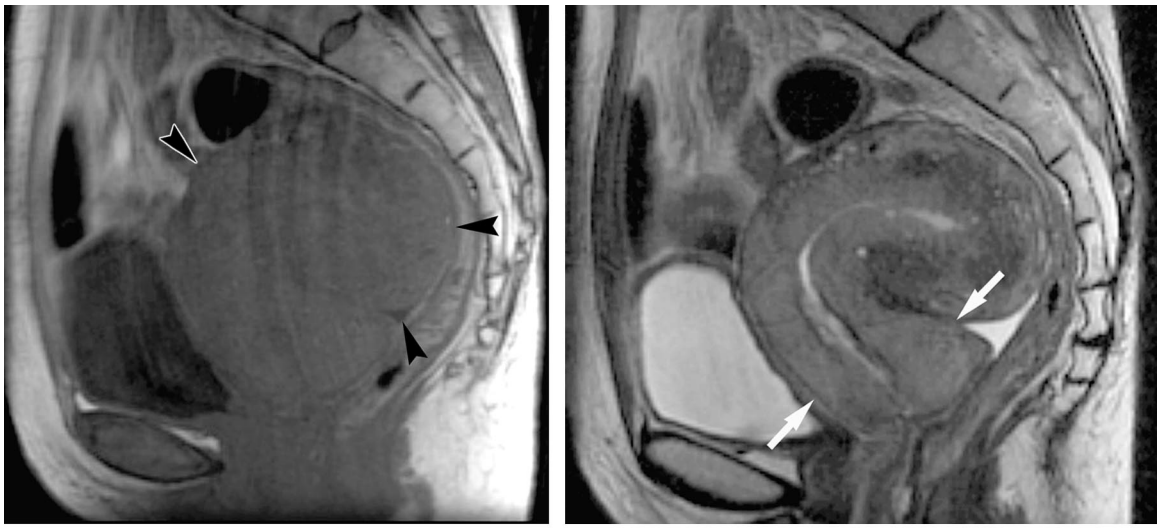

a. b.

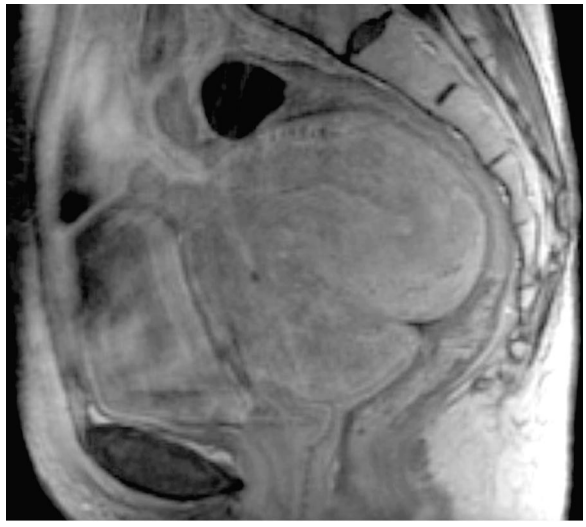

c.

Figure 18. Malignant lymphoma in a 48-year-old woman with multiple swollen lymph nodes in the paraaortic and supraclavicular regions. **(a)** Sagittal T1-weighted image shows extensive uniform enlargement of the uterus (arrowheads), which has homogeneous low signal intensity. **(b)** Sagittal T2-weighted image shows diffuse symmetrical enlargement of the uterus, especially of the cervix (arrows). The lack of signal in the cervical stroma is obvious. The myometrium also lacks its zonal appearance and has low signal intensity with an irregular contour. The cause of this signal intensity is unknown. **(c)** Sagittal contrast-enhanced T1-weighted image shows heterogeneous enhancement of the uterus. The diagnosis of malignant lymphoma was established by means of biopsy of a lymph node. The uterine lesion significantly decreased in size with chemotherapy and was considered to represent uterine involvement by lymphoma.

images and epithelial preservation (27) (Fig 18). As malignant uterine lymphoma has a fair prognosis if properly treated, accurate evaluation and diagnosis of the disease are essential (28,29). Since it is sometimes difficult to distinguish malignant lymphoma from other uterine malignancies with routine biopsy samples, imaging findings can be helpful in making the appropriate diagnosis.

Endometrial Stromal Sarcoma.—Endometrial stromal sarcoma originates from the endometrium but invariably exhibits extensive myometrial involvement that is either sharply demarcated or diffusely infiltrative (30). This entity is subdivided into low-grade stromal sarcoma and high-grade stromal sarcoma. Low-grade stromal sarcoma can be encountered even in the second decade of life. Moreover, the diagnosis is difficult to establish because, in general, the tumor cells are not sufficiently atypical to be accurately distinguished from benign endometrial stromal cells. In contrast, preoperative diagnosis of high-grade stromal sarcoma is readily established by microscopic examination of curettage material. An important diagnostic clue for low-grade stromal sarcoma is identification of bands of low signal intensity within the area of myometrial invasion, which is either sharply demarcated or diffusely infiltrative on T2-weighted images (30) (Fig 19). Extension along the vessels, fallopian tubes, or ligaments is another characteristic of the tumor. Needless to say, imaging studies play an important diagnostic role in endometrial stromal sarcoma, especially in the case of low-grade stromal sarcoma.

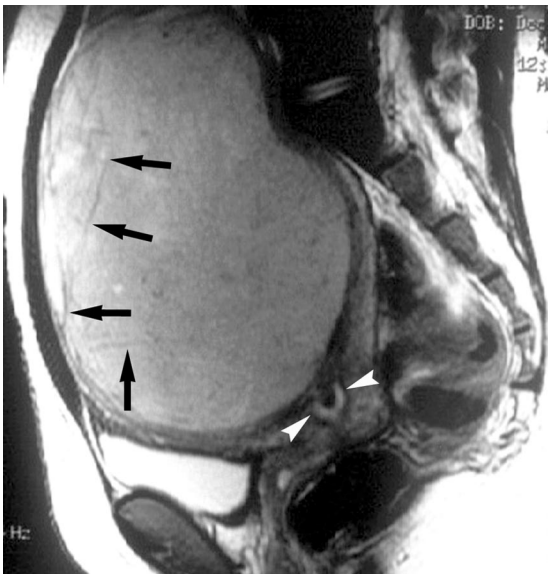

Figure 19. Low-grade endometrial stromal sarcoma in a 21-year-old woman. Sagittal T2-weighted image shows a huge tumor that replaces the endometrial cavity (arrowheads) and infiltrates the myometrium. Bands of low signal intensity (arrows) are seen in the infiltrated myometrium; these bands corresponded to preserved bundles of myometrium at histologic examination.

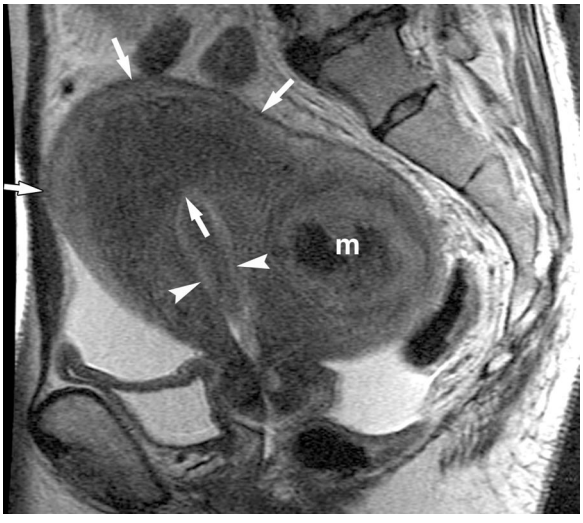

Figure 20. Uterine metastatic disease in a 51-year-old woman with abnormal genital bleeding who had undergone mastectomy for breast cancer. Sagittal T2-weighted image shows a diffusely thickened myometrium with low signal intensity (arrows) and a small amount of low-signal-intensity blood (arrowheads) in the uterine cavity. There is a leiomyoma *(m)* in the posterior wall. Cytologic analysis of endometrial tissue demonstrated metastatic adenocarcinoma from the breast tumor.

Other Uterine Malignancies.—Other malignancies may extensively involve the uterus in advanced stages, including cervical and endometrial cancers as well as mixed müllerian tumors. A diagnosis can be established from histologic samples obtained prior to imaging studies. Small cell carcinomas, which can arise from either the cervix or endometrium, are known for their propensity to spread rapidly and systemically and thus bear a poor prognosis. MR images demonstrate uniform uterine enlargement, which mimics the appearance of malignant lymphoma. Myometrial signal intensity is diffusely high on T2-weighted images (31).

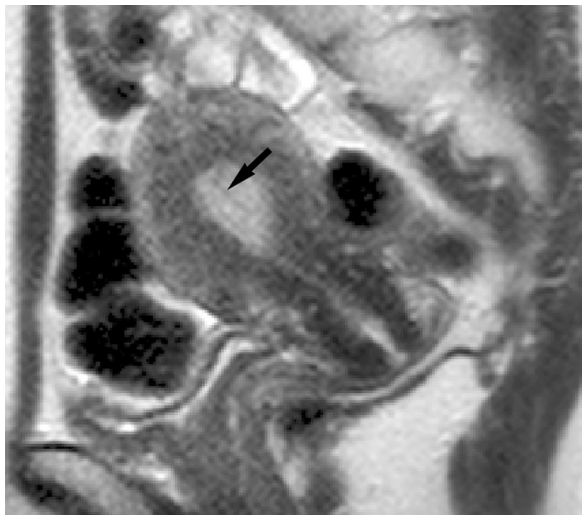

Figure 21. Uterine enlargement in a 41-year-old woman with an IUD that was placed 6 years earlier. Sagittal half-Fourier single-shot turbo spin-echo image shows a globular uterus. The IUD (arrow) is seen as a band of low signal intensity in the endometrium.

Uterine Metastatic Disease.—Metastatic disease to the uterus is rare; if present, it indicates a malignancy in an advanced stage (32). The most common primary sites are the breast and stomach. On MR images, the uterus appears enlarged. T2-weighted images exhibit abnormally high or low signal intensity throughout the myometrium (32,33) (Fig 20). Differentiating metastatic disease from hematologic diseases, such as lymphoma and leukemia, becomes difficult if the lesions exhibit high signal intensity. In contrast, when the lesions exhibit low signal intensity, a misdiagnosis such as adenomyosis can result.

Intrauterine Devices

Intrauterine devices (IUDs) are widely used for contraception. One study found that the IUD-bearing uterus is enlarged compared with the non–IUD-bearing state (34) (Fig 21). IUD

placement most likely results in myometrial hypertrophy. The associated findings are as follows: symmetrical globular enlargement of the uterine corpus, cervical elongation and enlargement, diffuse or localized myometrial thickening, individual myometrial cell hypertrophy, and muscle band broadening (34). The mechanism underlying such hypertrophy most likely stems from stimulation of prostaglandin release by the IUD. A chronic excess of prostaglandin $F_{2\alpha}$ might lead to progressive myometrial hypertrophy over time (34).

Conclusions

Diffuse uterine enlargement encompasses various conditions from physiologic changes to benign or malignant disease. MR imaging can provide valuable information regarding the myometrium in situations where it is difficult to obtain histologic samples, allowing differentiation of various diseases and establishment of specific diagnoses for many diseases.

Acknowledgments: The authors are grateful to Masato Noguchi, MD, Tadashi Sagoh, MD, Nobuyuki Kosaka, MD, Milliam Lika Kataoka, MD, and Christopher Jason Hurt, MD, for their valuable suggestions and assistance.

References

1. Silverberg SG, Kurman RJ. Tumors of the uterine corpus. In: Silverberg SG, Kurman RJ, eds. Tumors of the uterine corpus and gestational trophoblastic disease. 3rd ed. Washington, DC: Armed Forces Institute of Pathology, 1992; 1–2.
2. Fleischer AC, Kepple DM. Normal pelvic anatomy as depicted by various sonographic techniques. In: Fleischer AC, Javitt MC, Jeffrey RB, Jones HW III, eds. Clinical gynecologic imaging. Philadelphia, Pa: Lippincott-Raven, 1997; 10–41.
3. Garagiola DM, Tarver RD, Gibson L, Rogers RE, Wass JL. Anatomic changes in the pelvis after uncomplicated vaginal delivery: a CT study on 14 women. AJR Am J Roentgenol 1989; 153:1239–1241.
4. Willms AB, Brown ED, Kettritz UI, Kuller JA, Semelka RC. Anatomic changes in the pelvis after uncomplicated vaginal delivery: evaluation with serial MR imaging. Radiology 1995; 195:91–94.
5. Dicle O, Kucukler C, Pirnar T, Erata Y, Posaci C. Magnetic resonance imaging evaluation of incision healing after cesarean sections. Eur Radiol 1997; 7:31–34.
6. Negishi H, Kishida T, Yamada H, Hirayama E, Mikuni M, Fujimoto S. Changes in uterine size after vaginal delivery and cesarean section determined by vaginal sonography in the puerperium. Arch Gynecol Obstet 1999; 263:13–16.
7. Zuckerman J, Levine D, McNicholas MM, et al. Imaging of pelvic postpartum complications. AJR Am J Roentgenol 1997; 168:663–668.
8. Nalaboff KM, Pellerito JS, Ben-Levi E. Imaging the endometrium: disease and normal variants. RadioGraphics 2001; 21:1409–1424.
9. Nagayama M, Watanabe Y, Okumura A, Amoh Y, Nakashita S, Dodo Y. Fast MR imaging in obstetrics. RadioGraphics 2002; 22:563–580.
10. Demas BE, Hricak H, Jaffe RB. Uterine MR imaging: effects of hormonal stimulation. Radiology 1986; 159:123–126.
11. Azzopardi JG, Zayid I. Synthetic progestogen-oestrogen therapy and uterine changes. J Clin Pathol 1967; 20:731–738.
12. Ascher SM, Imaoka I, Lage JM. Tamoxifen-induced uterine abnormalities: the role of imaging. Radiology 2000; 214:29–38.
13. Sohaey R, Woodward P. Sonohysterography: technique, endometrial findings, and clinical applications. Semin Ultrasound CT MR 1999; 20: 250–258.
14. Malpani A, Singer J, Wolverson MK, Merenda G. Endometrial hyperplasia: value of endometrial

thickness in ultrasonographic diagnosis and clinical significance. J Clin Ultrasound 1990; 18:173–177.
15. Scully RE, Young RH, Clement PB. Sex cord-stromal tumors, granulosa cell tumors. In: Scully RE, Young RH, Clement PB, eds. Tumors of the ovary, maldeveloped gonads, fallopian tube, and broad ligament. 3rd ed. Washington, DC: Armed Forces Institute of Pathology, 1996; 169–188.
16. Huang MW, Muradali D, Thurston WA, Burns PN, Wilson SR. Uterine arteriovenous malformations: gray-scale and Doppler US features with MR imaging correlation. Radiology 1998; 206: 115–123.
17. Kido A, Togashi K, Koyama T, et al. Retained products of conception masquerading as acquired arteriovenous malformation. J Comput Assist Tomogr 2003; 27:88–92.
18. Dohke M, Watanabe Y, Okumura A, et al. Comprehensive MR imaging of acute gynecologic diseases. RadioGraphics 2000; 20:1551–1566.
19. Desimpelaere JH, Seynaeve PC, Hagers YM, Appel BJ, Mortelmans LL. Pelvic congestion syndrome: demonstration and diagnosis by helical CT. Abdom Imaging 1999; 24:100–102.
20. Coakley FV, Varghese SL, Hricak H. CT and MRI of pelvic varices in women. J Comput Assist Tomogr 1999; 23:429–434.
21. Reinhold C, Tafazoli F, Mehio A, et al. Uterine adenomyosis: endovaginal US and MR imaging features with histopathologic correlation. RadioGraphics 1999; 19:S147–S160.
22. Togashi K, Nishimura K, Itoh K, et al. Adenomyosis: diagnosis with MR imaging. Radiology 1988; 166:111–114.
23. Kuwashima Y, Uehara T, Kishi K, et al. Intramural adenocarcinoma of the uterus, arisen from adenomyosis uteri, showing unique histologic appearances: report of two cases. Eur J Gynaecol Oncol 1994; 15:418–423.
24. Hricak H, Tscholakoff D, Heinrichs L, et al. Uterine leiomyomas: correlation of MR, histopathologic findings, and symptoms. Radiology 1986; 158:385–391.
25. Ueda H, Togashi K, Konishi I, et al. Unusual appearances of uterine leiomyomas: MR imaging findings and their histopathologic backgrounds. RadioGraphics 1999; 19:S131–S145.
26. Worthington JL, Balfe DM, Lee JK, et al. Uterine neoplasms: MR imaging. Radiology 1986; 159: 725–730.
27. Kawakami S, Togashi K, Kojima N, Morikawa K, Mori T, Konishi J. MR appearance of malignant lymphoma of the uterus. J Comput Assist Tomogr 1995; 19:238–242.
28. Harris NL, Scully RE. Malignant lymphoma and granulocytic sarcoma of the uterus and vagina: a clinicopathologic analysis of 27 cases. Cancer 1984; 53:2530–2545.
29. Komaki R, Cox JD, Hansen RM, Gunn WG, Greenberg M. Malignant lymphoma of the uterine cervix. Cancer 1984; 54:1699–1704.
30. Koyama T, Togashi K, Konishi I, et al. MR imaging of endometrial stromal sarcoma: correlation with pathologic findings. AJR Am J Roentgenol 1999; 173:767–772.
31. Yamamoto T, Maeda M, Mori M, Itch H. MR imaging of small cell carcinoma of the uterus with associated inappropriate secretion of antidiuretic hormone. AJR Am J Roentgenol 2000; 174:1167–1168.
32. Kim SH, Hwang HY, Choi BI. Uterine metastasis from stomach cancer: radiological findings. Clin Radiol 1990; 42:285–286.
33. Nobusawa H, Gokan T, Hashimoto T, et al. Stage IIIa endometrial carcinoma: MR findings. Nippon Igaku Hoshasen Gakkai Zasshi 1996; 56:283–287. [Japanese]
34. Honore LH. Menorrhagia, diffuse myometrial hypertrophy and the intrauterine contraceptive device: a report of fourteen cases. Acta Obstet Gynecol Scand 1979; 58:283–285.

This article meets the criteria for 1.0 credit hour in category 1 of the AMA Physician's Recognition Award. To obtain credit, see accompanying test at http://www.rsna.org/education/rg_cme.html.